

## The WO stars

### III. The planetary nebula NGC 5189 and its O VI sequence nucleus\*

V.F. Polcaro<sup>1</sup>, C. Rossi<sup>2</sup>, R. Viotti<sup>1</sup>, and L. Norci<sup>3</sup>

<sup>1</sup> Istituto di Astrofisica Spaziale, CNR, C.P. 67, I-00044 Frascati RM, Italy

<sup>2</sup> Istituto Astronomico dell'Università "La Sapienza", Via G.M. Lancisi 29, I-00161 Roma, Italy

<sup>3</sup> Dunsink Observatory, Dublin Institute for Advanced Studies, Dublin, Ireland

Received 2 January 1996 / Accepted 27 June 1996

**Abstract.** Long slit blue and red spectra of the planetary nebula NGC 5189 (PK 307 -3°1) with its O VI sequence central object were obtained with the ESO 1.52 m telescope, in order to establish criteria that allow the discrimination between the high mass WO stars and lower mass objects having similar spectral features. The NGC 5189 stellar nucleus shows a very high ionization spectrum with emission features of He II, C IV, and O V. N V should also be weakly present. The line width suggests a maximum wind velocity of 2800 km s<sup>-1</sup>. Long slit spectra on various positions across the nebula were used to study the physical structure of NGC 5189. From the [S II] 671.7/673.2 nm line ratio we find that the electron density varies from 200 to 900 cm<sup>-3</sup>. The ionization, as described by the He<sup>++</sup>/He<sup>+</sup> ratio, largely changes from one region to another, reaching a maximum of 2.5 in a low density region 20''E of the central star, and a minimum in the regions more distant from the star. NGC 5189 appears nitrogen enriched by about a factor 5 with respect to the cosmic value, while the helium abundance is normal. The chemical composition appears homogeneous throughout the nebula. We thus conclude that, in addition to the wind velocity, the chemical composition and homogeneity of the nebulae can be used to discriminate between high mass WO stars and "O VI sequence" PNN's.

**Key words:** planetary nebulae – Wolf-Rayet stars – stars: individual: NGC 5189 PNN

---

#### 1. Introduction

The "O VI sequence" was first introduced by Smith and Aller (1969) to classify a small group of nuclei of Planetary Nebulae

*Send offprint requests to:* V.F. Polcaro, polcaro@saturn.ias.fra.cnr.it

\* Based on data collected at the European Southern Observatory, La Silla, Chile.

(PNN) showing a WR-type spectrum with strong O VI 381.1–383.4 nm emission. Later, Mendez and Niemela (1982) established a classification scheme for the WC central stars of planetary nebulae (PN) that includes the O VI central star sequence. Sanduleak (1971) described the spectra of five stars (now named Sand 1 to Sand 5) not surrounded by a PN, with similar spectral features. More recently, Barlow and Hummer (1982) argued that Sand 3 actually is an old PNN. In the same paper they introduced the "Population I WO" spectral class, grouping a few extreme, massive WR stars having their spectra dominated by the O VI 381.1–383.4 nm doublet and very high wind velocity and mass loss. It is a small spectral class: only 6 "Pop I WO" stars are up to date known in the Local Group (3 in our Galaxy, 1 in LMC, 1 in SMC and 1 in NGC 1613; Kingsburgh et al. 1995). This small number is a clear indication of the short time spent in this phase that, according to current models (e.g. Langer et al. 1994), is believed to be the latest evolutionary stage of very high mass stars ( $M_o > 40 M_\odot$ ). Thus, in order to avoid misidentifications that can strongly alter the statistics, it is important to establish solid criteria that allow the discrimination between these stars and objects having similar spectral features, such as the "O VI sequence planetary nuclei" (Stanghellini, Kaler & Shaw, 1994).

Thus, in the framework of a long term program devoted to the study of the massive WO stars (Polcaro et al. 1991; Polcaro et al. 1992, hereafter Paper I; Polcaro et al. 1995, hereafter Paper II), we decided to include in our observing programme also the nucleus of an O VI sequence PN in order to investigate the observable effects of different initial masses in stars with otherwise similar spectra.

The stellar nucleus of NGC 5189 (PK 307 -3°1) is one of the O VI sequence planetary nuclei. Mendez and Niemela (1982) classified this star as WC2 in their scheme. Its distance is evaluated to be  $\sim 1.5$  kpc and its temperature is very high (e.g., Kingsburgh and Barlow, 1994, and references therein). It has been widely studied in the past: more than 280 entries are reported under its name in the CDS/SIMBAD data base. On the other hand, most of the literature, apart from a few papers (e.g.

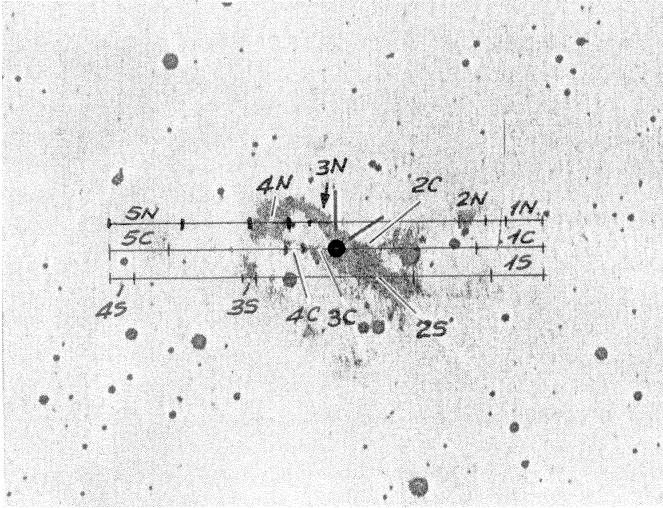


**Fig. 1.** The various slit positions are shown superimposed on the  $H\alpha$  image of NGC 5189 (from Blanco et al. 1968). The different regions of the nebula discussed in the paper are also indicated.

Blanco et al. 1968; Mendez 1991; Perinotto et al. 1994), reports physical parameters derived from spectroscopic observations integrated over the whole nebula, and often contaminated by the central star. The results of these investigations are useless for the purpose of a detailed comparison with the Pop I WOs, so that higher spatial and spectral resolution measurements were necessary. Actually, the spatially resolved study of the planetary nebula might in principle help to trace back the past history of the central star, as we have shown for the nebular matter around Sand 4 (Paper II), and can thus allow to discriminate between high mass and low mass objects, and to deeply understand their evolution. A preliminary summary of our results has been presented in Polcaro et al (1995b)

## 2. Observations and data analysis

We have obtained intermediate dispersion long slit spectra (0.08 and 0.10 nm  $\text{pix}^{-1}$ ) of NGC 5189 with the ESO 1.52 m telescope, equipped with B&C spectrograph and CCD detector. Observations were made on June 19-20, 1990, during the same observation run when we obtained the spectrum of Sand 4 and of its surrounding nebula (G2.4+1.4). The same 3'-long, East-West oriented slit was used for both cases, but, because of technical problems, NGC 5189 was observed only in two spectral ranges (blue: 432–487 nm, red: 616–723 nm). Three slit positions were selected (centred on the star, and  $\pm 10''$  in declination) in order to analyze the spectrum of the central "bar", and of the bright nebulosities around the central star, and some distant faint regions of the nebula. Fig. 1 shows the slit positions superimposed on the  $H\alpha$  image of NGC 5189 (from Blanco et al. 1968). The different regions of the nebula discussed in this paper (*n*1-5, *c*1-5, and *s*1-3) are also indicated. Table 1 reports the observations log. The spectrograms of the nebula were analyzed following the same procedures as described in Paper II.

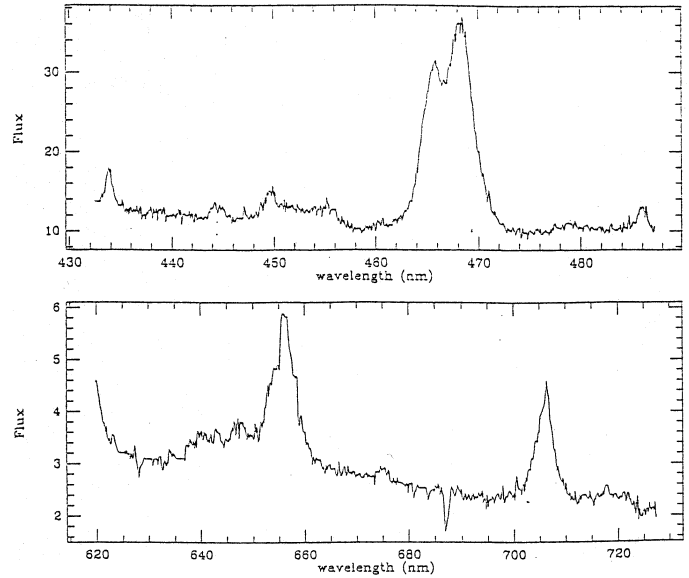


**Fig. 2.** The spectrum of the NGC 5189 central star. Top panel: blue range; bottom panel: red range. The spectrum is sky subtracted and flux calibrated. Ordinates are fluxes in  $10^{-14}$  erg  $\text{cm}^{-2}\text{s}^{-1}\text{nm}^{-1}$ .

## 3. The spectrum of the central star

The spectrum of the central star has been derived after a careful subtraction of the nearby sky and nebular spectrum. Nevertheless, the resulting spectrograms still contain nebular features, especially near 656 nm, which have been eliminated manually, but may still affect the line measurements reported in Table 2 below. A similar problem can be present in the 434 and 486 nm features, even though they have been fitted by double gaussians (a shallow one, probably of stellar origin, and a narrow, nebular one). Fig 2 a,b shows the sky and nebular subtracted stellar spectrum.

In Table 2 we report the line measurement and identification of the spectrum of the central star. The successive columns in the table give: (1) heliocentric peak, or central wavelength (in nm) of the measured feature; for not measurable features we give the laboratory wavelength in *italics*; colon: uncertain measure; (2) base width of the measured feature; (3) emission line equivalent width; colon: uncertain measure; "n.m.": present, but not measurable; (4) adopted local continuum level in  $10^{-8}$  W  $\text{m}^{-3}$  ( $10^{-15}$  erg  $\text{cm}^{-2}\text{s}^{-1}\text{nm}^{-1}$ ); (5) the observed line flux in  $10^{-18}$  W  $\text{m}^{-2}$ , (6) the line flux dereddened for  $E_{B-V}=0.32$  (see below); (7) line identification (ion, laboratory wavelength, transition); (8) remarks ("blend": broad blend of two or more lines; "main": main contributor to the blend; "contr": possible contributor to the feature; "?": uncertain identification; "n.i.": main contributor not identified).

For the line identification we have made use of Edlén (1956), the National Bureau of Standards publications NSRDS-NBS 3, Sects. 3, 4, and 9 (Moore 1970, 1980), the Atlas of the optical spectra of WC/WO stars of Torres and Massey (1987), and the works on the optical spectrum of the five Sanduleak's stars (e.g. Paper I and references therein), with particular attention to Sand

**Table 1.** Observation log of NGC 5189

date (1990)	slit position	exp. (min)	UT beg (hh:mm)	sp. range (nm)	res. (nm)
June 19*	on star (bC)	60	03:50	432–487	0.10
June 19	10''N (bN)	60	04:34	432–487	0.10
June 20*	on star (rC)	20	00:54	616–723	0.19
June 20*	10''N (rN)	30	01:20	616–723	0.19
June 20	10''S (rS)	20	01:43	616–723	0.19

**Table 2.** The June 1990 spectrum of the central star of NGC 5189

OBS WL (1)	WID (2)	EQW (3)	CONT (4)	F <sub>i</sub> (5)	F <sub>i</sub> <sup>o</sup> (6)	ION (7)	REMARKS (8)
433.9	2.8	0.42:	127	53	178	He II 433.9 (10-4) C IV 433.8 (20-8) O VIII 434.0 (9-8)	neb, main
444.4	2.8	0.24	115	28	91	C IV 444.0, 444.1 m4 (6d-5p) O V 444.7 m21 (7h-6g)	main contr
449.6	3.5	0.53	113	60	192	O V 449.8 m22 (7h-6g) O VI 449.9 (10-8)	main
452–455	4.8	1.5	104	156	560	O V 452.3 m15 (3d'-3p') O V 452.2 (9-7) C V 452.0 (9-7) He II 454.1 (9-4) O V 455.4 m7 (3d'-3p') O VII 455.6 (11-9)	main contr contr main contr contr
460.8:		n.m.				N V 460.3 m1 (3p-3s)	?, weak
465.8	8	6.6		660	2030	C IV 465.8 (6h-5g)	main
468.3	11.1	11.2		1120	3420	He II 468.6 (4-3) C IV 468.5 (8-6)	neb, main contr
478.8:		n.m.				C IV 478.6, 8.7 m5 (6p-5d) O IV 477.9-478.9 m9 (3d-3p)	weak ?, contr
485.9	3.0	0.45	111	55	160	He II 485.9 (8-4) C IV 485.9 (16-8)	neb, main contr
620.1		n.m.				O VI 620.2 (11-9, 13-10) C III 602.5 m16 (5s-4p) He II 617.1 (17-125) He II 623.4 (15-16)	main contr contr contr
640.8		n.m.				C IV 640.8 (17-9) He II 640.6 (15-5)	weak
646.8:		n.m.				O V 646.0, 646.6 (3d'-3p')	weak
650.0		n.m.				O V 650.0 (3d'-3p')	
656.0	10.6	3.8	28	107	222	C IV 655.9 (12-8) He II 656.0 (6-4)	neb, contr contr
674.6::	4.	0.17:	26	5	9	C IV 674.7 (16-9) C III 674.4 (3d-3p)	weak ? contr
705.8	11.1	3.6	23	85	163	C IV 706.2 (9-7)	
717.7::		n.m.				He II 717.7 (11-5)	weak
721.0::		n.m.				C IV 720.7 (15-9)	weak

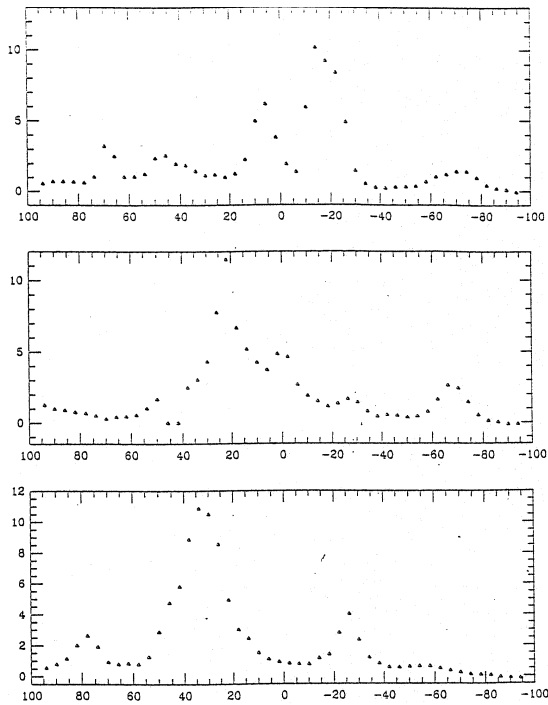


**Fig. 3.** Flux variation of H $\alpha$  brightness versus distance along the three slits. Abscissae are arcsec from the right ascension of the central star. East is towards the left. Ordinates are fluxes in  $10^{-13}$  erg cm $^{-2}$ s $^{-1}$  per 6 arcsec $^2$ . Top: 10'' N; Center: on the PNN; Bottom: 10'' S

3 (Barlow et al. 1980), which has a spectrum very similar to that of the central star of NGC 5189. We also used the Werner et al (1990), Werner and Heber (1991 a,b) papers on the PG1159 stars.

The following emission features have been identified.

– 433.9 nm Weak emission wings on the H $\gamma$  nebular emission line, extending from the short wavelength edge of the spectrum to 434.8 nm. This line could be attributed to a blend of He II, C IV, O VIII. The line is too strong in comparison with the  $\lambda 454.1$  line of the same Brackett series to be attributed only to He II (even though probably the measured flux is overestimated). The expected contribution of C IV should be small. The possible identification of O VIII needs to be supported by larger S/N spectrophotometry and by observations of other transitions of this ion in spectral regions not covered by our observations, such as the  $\lambda 606.42$ – $606.82$  doublet which has been observed in the massive WO star Sand 4 (Paper I).

– 444.4 Weak emission of C IV also present in Sand 3.

– 449.–455. Broad emission blend extending from 448.1 nm to 457.5 nm, which is attributed to the blending of many O V and He II lines; O VI  $\lambda 449.9$ , C V  $\lambda 452.0$ , and O VII  $\lambda 455.6$  may also contribute to the blend.

– 460.8 Very weak feature also present in Sand 3 and attributed by Barlow et al. (1980) to N V  $\lambda \lambda 460.37, 462.0$  (m1), which is the strongest unblended transition of this ion in the optical spectra of early type WN stars. The feature appears as an extension of the short wavelength wing of the strong 468 nm emission.

– 465.8–468.3 Very strong broad emission extending from  $\sim 461.2$  nm to 472.7 nm, with two peaks at 465.8 nm (C IV  $\lambda 465.8$ ), and at 468.3 nm (He II  $\lambda 468.6$ ). The flux of each component has been derived by means of a double Gaussian fit of the blend. C IV  $\lambda 468.5$  should give a minor contribution to the second component. We cannot exclude the contribution of the C III  $\lambda 465.0$  and  $\lambda 466.6$  nm; this point will be further analyzed later.

– 485.9 Weak emission wings of the nebular emission line, extending from  $\sim 484.6$  nm to the long wavelength edge of the spectrum. He II  $\lambda 485.9$  should be the main contributor, although its strength is somewhat larger than expected as compared to the 454.1 line, due to the uncertainty in the line flux, as discussed above for  $\lambda 433.8$ .

– 620.1 Strong emission cut by the short wavelength edge of the spectrum, and extending to  $\sim 623.9$  nm. The emission is present in the PNN Sand 3 and in the WO star Sand 4. C III  $\lambda 620.5$  nm and He II  $\lambda 617.1$  and  $\lambda 623.4$  nm could be present but we consider the main contributor to this line a blend of the O VI (11–9, 13–10)  $\lambda 620.2$  nm as suggested by Kingsburgh et al. (1995) in their study of massive WO stars.

– 640.8 Weak emission attributed to He II. C IV 17-9 probably contributes to the line, as the 16-9 (674.7 nm), and 15-9 (720.7 nm) transitions coincide with two weak humps in the red spectrum.

– 646.8, 650.0 Weak emissions identified with the O V  $3d^3F$ – $3p^3D$  multiplet (Edlén 1956, Torres and Massey 1987).

– 656.0 Broad and intense emission extending from 649.8 nm to 661.3 nm. The measured flux is affected by the difficult subtraction of the nebular lines. The main contributors are C IV  $\lambda 655.9$  and He II Br $\beta$ .

– 674.6 Weak emission hump attributed to the C IV  $\lambda 674.4$  (16-9) transition.

– 705.8 Moderately intense emission extending from 700.3 nm to 711.7 nm, due to the strong C IV  $\lambda 706.2$  9-7 transition.

– 717.6 Weak emission identified with He II  $\lambda 717.7$ .

– 721.0 Weak hump of the spectrum, blended with the  $\lambda 717.6$  emission, probably due to the C IV 720.7 (15-9) transition.

The main emission features extend from  $-2800 \pm 200$  km s $^{-1}$  to  $+2500 \pm 200$  km s $^{-1}$ , which correspond to a maximum wind velocity much smaller than that measured in the WO stars Sand 1 (4200 km s $^{-1}$ , Kingsburgh and Barlow 1995), Sand 4 (4600–6600 km s $^{-1}$ , Paper I) and Sand 5 (5500 km s $^{-1}$ , Polcaro et al. 1991), but comparable with the velocity of 2700 km s $^{-1}$  found in Sand 3 (Barlow et al. 1980).

The optical spectrum of the central star of NGC 5189 is dominated by He II, C IV, and O V, like the spectrum of Sand 3 (Barlow et al. 1980, Barlow and Hummer 1982). Higher ionization stages of oxygen, such as O VI, and O VII, might also be present in our spectrum, although higher S/N observations are required to confirm this. This can also be the case of O VIII that is probably contributing 433.8 nm blend. In this respect, observations in wavelength ranges different from those used in this study would be of course desirable.

Lower excitation species, as O IV and C III, should also be present, but their presence is unnecessary in order to explain most of the stellar features (as is the case of the 465.6-468.3 blend). Actually, the C III  $\lambda$ 620.6 nm could be responsible for the unidentified 620.1 nm line. But the presence of the feature in most of the massive WO stars makes this identification highly unreliable.

Of special interest is the identification of the N V  $\lambda$ 460.3-462.0, which belongs to the same isoelectronic sequence of C IV  $\lambda$ 580.1–581.2, and O VI  $\lambda$  381.1–383.4, which are the strongest emission lines in the spectra of early-type WO/WC stars. If this identification is valid, this could indicate that the atmosphere of this star is not completely deprived of nitrogen.

On the other hand, small humps at the same wavelength seem to be present on the blue wing of the very strong blend C IV and He II in the massive WO Sand 4 and Sand 5 (see Fig 1 of Paper I and Polcaro et al 1991), where the presence of Nitrogen is quite difficult to explain.

The PNN continuum (once dereddened with an  $E_{B-V}=0.32$ ) is fitted by the Raleigh-Jeans tail of a very hot ( $T>100$  kK) black-body.

The similarity between the spectra of the central star of NGC 5189 and of Sand 3, and the absence of a bright nebulosity around the latter Sand 3 (which should anyhow deserve new deeper observations) should indicate that the "O VI sequence" phase of a PNN lasts longer than the PN lifetime.

#### 4. Long slit spectra of the Planetary Nebula

The blue and red spectral images of NGC 5168 were analysed in order to study in detail the spatial distribution of the emission line brightness. The line brightness is largely variable across the nebula, with many regions of enhanced emissivity. The "knotty" structure is quantitatively described in Fig.3 which shows the H $\alpha$  brightness variation along the three slits. From the plots we have identified 13 regions of maximum emission, which were selected for the following study of the nebular parameters.

In addition to the hydrogen lines, many emissions are present, namely: He I  $\lambda$ 447.1, 471.3, 667.8, 706.4; He II  $\lambda$ 454.1, 468.6, 689.1, 717.7; [O I]  $\lambda$ 630.0, 636.3; [O III]  $\lambda$ 436.3; [N II]  $\lambda$ 654.8, 658.4; N III  $\lambda$ 463.4, 464.0; [S II]  $\lambda$ 671.7, 673.1; [S III]  $\lambda$ 631.0; [Ar III]  $\lambda$ 713.5; [Ar IV]  $\lambda$ 471.1, 474.0; [Ar V]  $\lambda$ 649.5, 700.6; [Ne IV]  $\lambda$ 472.5; [Fe III]  $\lambda$ 465.8. Some of these lines (eg. N III and [Fe III]) are very weak and are seen only in the brightest regions. The He I 471.3 nm line is very weak and blended with [A IV]  $\lambda$ 471.1; the peaks of the two lines are well separated in those regions where [A IV] is faint.

We have measured the average line intensity in the above selected nebular regions. The relative intensities of the dereddened lines fluxes are reported in Table 3 and the derived the nebular parameters are given in Table 4. It is evident from our data that, while the values averaged over the whole nebula are in perfect agreement with those reported in the literature (e.g. Stanghellini et al. 1995), many physical parameters appear highly non homogeneous.

For the electron density we have used the intensity ratio of the [S II] red doublet. Assuming an electron temperature of  $T_e=13100^\circ K$ , (as derived by Kingsburgh & Barlow, 1994, from the [O III]) we have found that  $N_e$  largely varies across the nebula, with values ranging, in the brightest parts of it, from 200 to 900  $\text{cm}^{-3}$ , reaching the largest values along the "bar" (regions, from NE to SW, 4n, 3n, 3c, 2c, and 2s). Previous studies of NGC 5189 have provided "mean" electron densities – derived from line fluxes integrated over the nebula – of 680  $\text{cm}^{-3}$  (from [O II], Kingsburgh & Barlow 1992),  $390\pm 60$   $\text{cm}^{-3}$  (from [S II], Kingsburgh & Barlow 1994), 600 to 800  $\text{cm}^{-3}$  (three regions of NGC 5189, Perinotto et al. 1994) and 700  $\text{cm}^{-3}$  (Stanghellini et al. 1995).

The ratio of the [Ar IV] 471, 474 nm lines is a good density indicator for  $N_e$  ranges higher than those which can be investigated using the [S II] red doublet. As said above, the  $\lambda$ 471.1 line is blended with He I  $\lambda$ 471.3, but the resolution of our spectrograms has enabled us to separate the blend fairly well, by means of a double Gaussian fit. In the higher ionization regions, the He I line is much weaker, and contributes to the red wing of the [A IV] line, while in the lower ionization knots the two line have comparable strength, and have emission peaks fairly well separated. In these regions, the 471.3/474.1 flux ratio is close to 0.2, to be compared with the theoretical ratio of 0.1 for a  $T_e=10000^\circ$ ,  $N_e=10000$   $\text{cm}^{-3}$  plasma. After having removed the contribution of the He I line, from the [A IV] flux ratio we have obtained  $N_e=3100$   $\text{cm}^{-3}$  for knots 2c, 3n and 4n, 4200  $\text{cm}^{-3}$  for 1n and 2n, and  $N_e=4000$   $\text{cm}^{-3}$  for 3c; for 4c we have obtained a low density limit. In the other nebular structures the [Ar IV] lines are not detectable. These  $N_e$  estimates are definitely higher than those derived for the same knots from the [S II] red doublet ratio. This result is not uncommon in the study of Planetary Nebulae. For instance, Kingsburgh and Barlow (1994) systematically derived from [A IV] densities much higher than those obtained from the [S II] data. The apparent contradiction can be explained by supposing the presence of density gradients inside the nebular knots, as suggested by Panagia and Preite Martinez (1975). In this hypothesis, the [Ar IV] densities are related to the inner and denser parts of the structures, while the [S II] red lines are referred to the outer more tenuous parts, where these lines are mostly formed.

As for the interstellar extinction is concerned, since H $\alpha$  and H $\beta$  have been recorded on different images obtained in different nights, we have preferred to use the more homogeneous H $\gamma$ /H $\beta$  ratio. This ratio appears constant within the errors, with a mean value of  $0.41\pm 0.03$  which, if compared with the Case B,  $T_e=10000^\circ K$  value of 0.47, corresponds to  $E_{B-V}=0.32^{+0.16}_{-0.20}$ , in good agreement with the  $c(H\beta)$  values of 0.49 and 0.56 ( $E_{B-V}=0.33$  and 0.38), as derived from the comparison of radio and H $\beta$  integrated fluxes (Kingsburgh & Barlow 1992, Kingsburgh & Barlow 1994). We adopted the  $E_{B-V}$  value of 0.32 to correct the observed stellar and nebular fluxes.

Assuming  $T_e=13100^\circ K$  and the [S II] electron densities, we have derived the ionic abundances in the different regions given in Table 4. The He<sup>+</sup> abundance has been determined from the He I  $\lambda$ 447 and  $\lambda$ 668, taking into account the C/R correction

factors (from Clegg 1987). We also assume negligible neutral helium abundance. It turns out from the table that the ionization degree, as indicated by the  $\text{He}^{++}/\text{He}^+$  ionic ratio, is largely variable throughout the nebula, reaching the highest values in regions rather distant from the central star ( $2n$ ,  $5n$ ), and, especially in the low density region  $4c$ ,  $20''\text{E}$  of the star. The ionization is also quite low in the distant eastern nebulousity  $5c$ .

The helium abundance is within the observational errors uniform throughout the whole nebula, as expected, and has a mean value of  $\text{He}/\text{H} = 0.10 \pm 0.01$ , in agreement with the Planetary Nebulae median value of 0.115 (Pottasch 1983, see also Kingsburgh et al. 1994). (The  $\text{He}^+/\text{H}$  abundance in region  $4c$  is uncertain because of the weakness of the  $\text{He I}$  lines).

As in Paper II we have estimated the nitrogen abundance from the  $[\text{N II}]/[\text{S II}]$  red doublets ratio. The derived  $\text{N}^+/\text{S}^+$  values are reported in Table 3, and are strongly suggestive of a large nitrogen overabundance with respect to  $\text{H II}$  regions and, especially with respect to the cosmic value. The mean value of  $1.49 \pm 0.05$  (excluding the  $\text{N}^+/\text{S}^+$  ratio of region  $4c$ ), is three times larger than that found in the  $\text{H II}$  nebula G2.4+1.4 surrounding Sand 4 (Paper II), and five times the cosmic  $\text{N}/\text{S}$  (Allen 1973).

## 5. Comparison with Sand 4 and conclusion

The comparison between the spectra of O VI sequence PNNs and "Pop I WOs" is necessary to discriminate between low and high mass stars in order to provide classification criteria for any new object with a circumstellar nebula exhibiting a spectrum characterized by strong O VI  $\lambda$  381.1-383.4 nm. Furthermore the comparison is a useful mean to investigate how the initial mass affects the last stages of the stellar evolution.

As for the central objects, our analysis (to our knowledge performed with spatial and spectral resolution higher than those published up to date) while confirming known differences, has added some new discriminating tools.

We confirmed the differences between Sand 4 (representing the class of Pop I WOs) and the central object of NGC 5189 in the line widths, that are definitely smaller in the PNN. For this reason many more lines appear separated in the NGC 5189 PNN than in Sand 4, allowing a more accurate and complete identification. In addition, while the main features are the same in the two stars, our analysis showed differences in the ionization levels of the atomic species. The blend of O V, O VI, and He II between 449 and 456 nm, that gives a single shallow profile in the spectrum of Sand 4, shows three well separated peaks corresponding to O V + O VI  $\lambda$  449.9, He II  $\lambda$  454.16, and O V  $\lambda$  455.45. Note that the NGC 5189 PNN has a Zanstra temperature evaluated as  $\sim 130$  kK (Perinotto et al. 1994), while for Sand 4 the temperature is  $\sim 80$  kK (e.g. Paper I and references therein).

As for the circumstellar matter, our study gives many new interesting results. One difference that was not noticed before, is that no significant circumstellar reddening is present in the NGC 5189 PNN, while a strong reddening excess was measured around Sand 4 with respect to its nebula (Paper II).

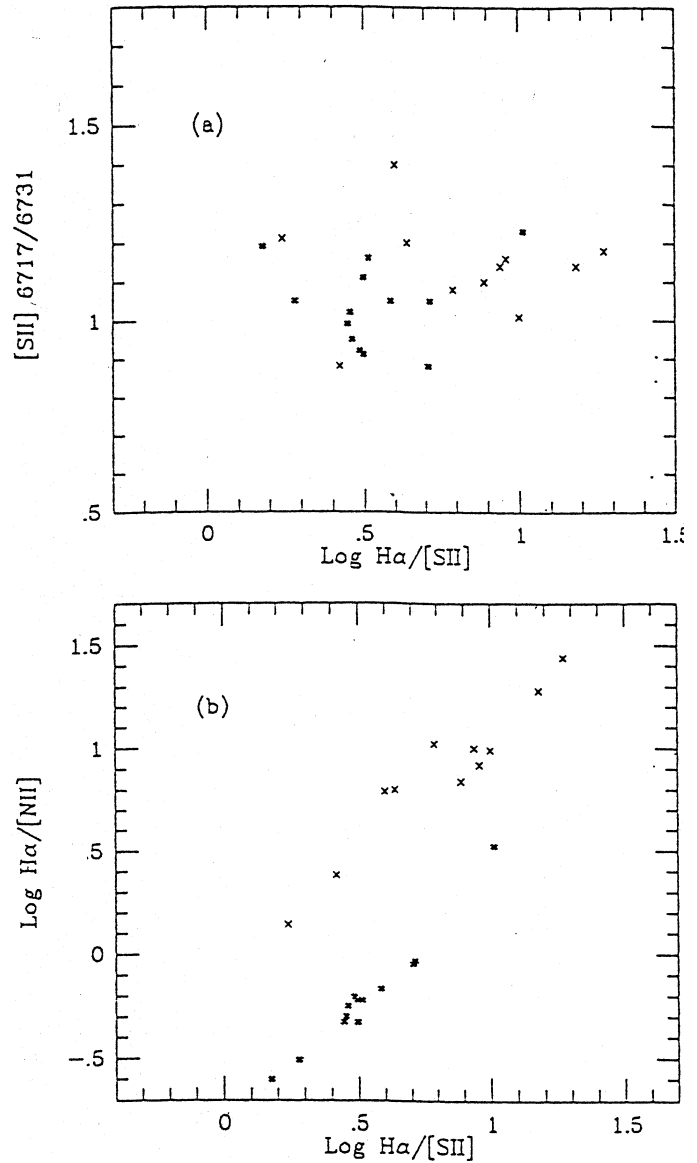


**Fig. 4.** Diagnostic diagrams for NGC 5189 (*stars*) compared with the G2.4+1.4 nebula from paper II (*crosses*), data from Esteban et al. (1992, *squares*).

Furthermore, the comparison of the nebular spectra of NGC 5189 and G2.4+1.4 shows that both have a large spread in the He ionization, but the general ionization level is definitely higher in NGC 5189, as proven by the presence of the  $[\text{Ar IV}]$  lines and of many He II lines that are below the detection level in our spectra of G2.4+1.4. This higher ionization of NGC 5189 might be associated with the higher temperature of the central star, and to the physical structure of the circumstellar nebula. To better discuss the matter of the abundances in the two nebulae we have chosen the diagnostic diagrams shown in figs. 4 and 5.

Fig. 4a shows the  $[\text{S II}] 671.7/673.2$  vs  $\log \text{H}\alpha/[\text{S II}]$  diagram (where  $[\text{S II}]$  is the sum of the flux in the 671.7, 673.2 nm lines). In the figure the data points of NGC 5189 and of the G2.4+1.4 nebula data are plotted. Notice the large spread in the  $\text{H}\alpha/[\text{S}]$

**Table 3.** Dereddened flux ratios in selected regions of NGC 5189

flux ratios	1n	2n	3n	4n	5n	1c	2c	3c	4c	5c	1s	2s	3s
$H\gamma/H\beta$	0.44	0.48	0.46	0.44	0.50	0.53	0.46	0.48	0.47	0.30	==	==	==
HeI 447/ $H\beta$	.030	==	.021	.027	==	==	.031	.032	.035	.0061	==	==	==
HeI 468/ $H\beta$	0.38	0.73	0.54	0.48	0.83	0.40	0.44	0.52	0.22	0.56	==	==	==
[NII]/ $H\alpha$	1.45	1.07	1.91	1.14	1.66	2.14	1.74	2.00	4.01	0.30	3.22	1.71	2.10
HeI 668/ $H\alpha$	.0067	.0062	.0098	.0087	.0067	.0071	.0119	.0097	.0089	.0033	.0097	.0106	.0089
[SII] 6717/31	1.06	1.05	0.95	0.88	1.17	1.12	0.92	1.03	1.21	1.23	1.05	0.93	0.99
[SII]/ $H\alpha$	0.26	0.19	0.35	0.20	0.31	0.32	0.32	0.35	0.67	0.097	0.53	0.33	0.50

**Table 4.** Physical parameters of NGC 5189

region (Fig.1)	$\log N_e$ ([S II])	He <sup>++</sup> /H $\lambda 468$	He <sup>+</sup> /H $\lambda 447$	He <sup>+</sup> /H $\lambda 668$	He/H	He <sup>++</sup> /He <sup>+</sup>	$\log$ N <sup>+</sup> /S <sup>+</sup>	remarks
1n	2.71	.033	.064	.049	.09	0.6	1.50	
2n	2.71	.063	n.m.	.045	.11	1.4	1.50	
3n	2.88	.046	.044	.071	.10	0.8	1.45	close to star
4n	3.01	.042	.055	.062	.10	0.7	1.50	high $N_e$
5n	2.50	.071	n.m.	.051	.12	1.4	1.50	
1c	2.59	.034	n.m.	.053	.09	0.6	1.59	
2c	2.95	.038	.064	.086	.11	0.5	1.46	close to star
3c	2.76	.045	.066	.070	.11	0.7	1.51	close to star
4c	2.33	.048	.013	.022	.07:	2.7	1.26	high ion., low $N_e$
5c	2.43	.019	.075	.066	.09	0.3	1.55	low ion.
1s	2.71	n.m.	n.m.	.070			1.54	
2s	2.93	n.m.	n.m.	.076			1.45	high $N_e$
3s	2.82	n.m.	n.m.	.065			1.38	

II] of NGC 5189 ratio, similar to that found in G2.4+1.4. This is associated with the wide density spread in both nebulae. We also notice that the density ranges in NGC 5189 and G2.4+1.4 are quite similar.

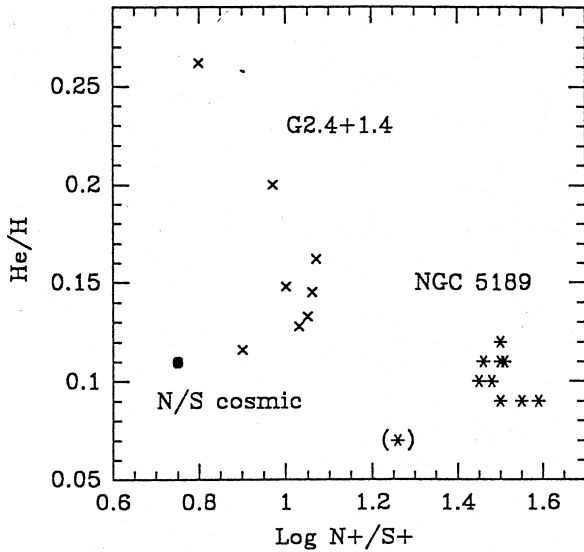
Fig. 4b gives the diagram  $\log H\alpha/[N II]$  vs  $\log H\alpha/[S II]$  for the two nebulae. The points of the PN are distributed approximately along a 45 degrees line shifted towards lower  $\log H\alpha/[N II]$  values than those of the Sand 4 nebula. This suggests a nitrogen overabundance (relative to sulfur) of the PN with respect to the nebula around the more massive star.

Fig.5 shows the He/H vs N<sup>+</sup>/S<sup>+</sup> diagram. We see that the chemical composition of the two nebulae is markedly different, possibly because of the different processes experienced in the evolution of their central objects. Actually, NGC 5189 has helium abundance normal and nitrogen enriched with respect to the cosmic composition; conversely in G2.4+1.4 the abundances vary, moving across the nebula from regions farther from the central star to the nearest ones, following a narrow strip which starts from the representative point of the cosmic He/H, N/S values and increases towards high He/H and high N/S up to a maximum; it then bends to lower N/S and higher He/H values (Paper II). As discussed in Paper II, this behaviour should mark

the different evolutionary phases of the central star. The absence of such an abundance spread in NGC 5189 indicates that the planetary nebula was formed during a single evolutionary phase, while in G2.4+1.4 it is the result of a complex evolutionary path.

On the basis of our measurements, the morphology of NGC 5189 appears to be probably of the "hour glass" type, the "bar" being the projection of a ring seen edge-on. Actually, our analysis clearly shows that the whole region surrounding the central object is filled up by matter having basically the same composition, so that the different emissivity is most probably due mainly to density gradients and ionization effects. Since also the G2.4+1.4 morphology can be explained by a bipolar structure (see Paper II and references therein) we want to suggest the presence of similar fluidodynamical interactions (e.g. Pascoli 1992) between stellar winds, stellar ejecta and interstellar matter, in spite of different chemical composition.

*Acknowledgements.* We thank Dr A. Preite Martinez (CNR-IAS) and Dr L. Stanghellini (OAB) for useful discussions. We also thank K. Weber (Univ. of Kiel) for providing us with a list of transitions of high ionization species. This work has made use of the SIMBAD database at the CDS (Strasbourg). The reduced ESO spectrograms of NGC 5189



**Fig. 5.** The He/H vs.  $N^+/S^+$  abundance ratio in different regions of NGC 5189 (stars) and G2.4+1.4 (crosses).

listed in Table 1 are available as computer ASCII files on request to the authors at the INTERNET address polcaro@saturn.ias.fra.cnr.it or rossic@axrma.uniroma1.it

## References

- Allen C.W. 1973, *Astrophysical Quantities*, The Athlone Press, University of London
- Barlow M.J. 1991, *Wolf-Rayet Stars and Interrelations with Other Massive Stars in Galaxies*. In: van der Hucht K.A., Hidayat B. (eds.) Proc. IAU Symp. 143, Kluwer, Dordrecht, p.281
- Barlow M.J., Blades J.C., Hummer D.C. 1980, ApJ 241, L27
- Barlow M.J., Hummer D.C. 1982, *Wolf-Rayet Stars: Observation, Physics, Evolution*. In: de Loore C.W.H. & Willis A.J. (eds.) Proc. IAU Symp. 99, Reidel, Dordrecht, p.387
- Blanco V., Kunzel W., Hiltner W.A. et al. 1968, ApJ 152, L135
- Blair W.P., Long K.S., Vancura O. 1991, ApJ 366, 484
- Clegg R.E.S. 1987, MNRAS 229, 31p
- Edlén 1956, *Vistas in Astronomy Vol.2*, p.1456
- Esteban C., Vilchez J.M., Smith L.J., Clegg R.E.S. 1992, A&A 259, 629
- Kingsburgh R.L., Barlow M.J. 1992, MNRAS 257, 317
- Kingsburgh R.L., Barlow M.J. 1994, MNRAS 271, 257
- Kingsburgh R.L., Barlow M.J., Storey P.J. 1995, A&A 295, 75
- Langer N., Hamann W.-R., Lennon M., et al. 1994, A&A 290, 819
- Mendez R.H. 1991, *Evolution of stars*. In: G. Michaud and A. Tutukov (eds.) Proc. IAU Symp. 145, Kluwer, Dordrecht, p. 375
- Mendez R.H. & Niemela V., 1982, *Wolf-Rayet Stars: Observation, Physics, Evolution*. In: de Loore C.W.H. & Willis A.J. (eds.) Proc. IAU Symp. 99, Reidel, Dordrecht, p. 457
- Moore Ch.E. 1970-1980, National Bureau of Standards, NRSD-NBS 3, Sects. 3, 4, 9
- Panagia N., Preite Martinez A. 1975, A&A 43, 93
- Pascoli G. 1992, PASP 104, 350
- Perinotto M., Purgathofer A., Pasquali A., Patriarchi P. 1994, A&AS 107, 481
- Polcaro V.F., Rossi C., Norci L., et al., 1991, A&A 252, 590
- Polcaro V.F., Viotti R., Rossi C., Norci L. 1992, A&A 265, 563 (Paper I)
- Polcaro V.F., Viotti R., Rossi C., Norci L. 1995, A&A 303, 211 (Paper II)
- Polcaro V.F., Viotti R., Rossi C., Norci L. 1995b, Proc of the Ven Workshop on "Planetary Nebulae with WR Nuclei", Ven, August 18-25 1995, *in press*
- Pottasch S.R. 1982, *Planetary Nebulae*, D. Reidel, Dordrecht, The Netherlands
- Sanduleak N. 1971, ApJ 164, L71
- Stanghellini L., Kaler J.B., Shaw R.A. 1994, A&A 291, 604
- Stanghellini L., Kaler J.B., Shaw R.A., di Serego Alighieri S. 1995, A&A 302, 211
- Smith L.F., Aller L.H. 1969, ApJ 157,1245
- Torres A.V., Massey P. 1987, ApJS 65, 459
- Werner K., Heber U., Hunger K. 1990, A&A, 244, 437
- Werner K., Heber U. 1991a, A&A, 244, 437
- Werner K., Heber U. 1991b, Proc of the Kiel/CCP7 Workshop on "Atmospheres of Early-type Stars", Sept. 18-20, 1991, Springer, p.291